

GeoRA: Geometry-Aware Low-Rank Adaptation for RLVR

Jiaying Zhang^{1,2†*}, Lei Shi^{1*}, Jiguo Li¹,
 Jun Xu^{1‡}, Jiuchong Gao^{1‡}, Jinghua Hao¹, Renqing He¹

¹Meituan, ²Peking University

{xujun58, gaojiuchong}@meituan.com

Abstract

Reinforcement Learning with Verifiable Rewards (RLVR) is crucial for advancing large-scale reasoning models. However, existing parameter-efficient methods, such as PiSSA and MiLoRA, are designed for Supervised Fine-Tuning (SFT) and do not account for the distinct optimization dynamics and geometric structures of RLVR. Applying these methods directly leads to spectral collapse and optimization instability, which severely limit model performance. Meanwhile, alternative approaches that leverage update sparsity encounter significant efficiency bottlenecks on modern hardware due to unstructured computations. To address these challenges, we propose GeoRA (Geometry-Aware Low-Rank Adaptation), which exploits the anisotropic and compressible nature of RL update subspaces. GeoRA initializes adapters by extracting principal directions via Singular Value Decomposition (SVD) within a geometrically constrained subspace while freezing the residual components. This method preserves the pre-trained geometric structure and enables efficient GPU computation through dense operators. Experiments on Qwen and Llama demonstrate that GeoRA mitigates optimization bottlenecks caused by geometric misalignment. It consistently outperforms established low-rank baselines on key mathematical benchmarks, achieving state-of-the-art (SOTA) results. Moreover, GeoRA shows superior generalization and resilience to catastrophic forgetting in out-of-domain tasks.

1 Introduction

Large reasoning models, represented by OpenAI-o1 (Jaech et al., 2024) and DeepSeek-R1 (Guo et al., 2025), have established Reinforcement Learning with Verifiable Rewards (RLVR) as a pivotal paradigm for unlocking complex reasoning

capabilities. Distinctively, RLVR exhibits the dynamics of a constrained optimization process (Wu et al., 2025), primarily amplifying latent reasoning behaviors via reward-induced sampling bias (Yue et al., 2025; Zhao et al.). This makes the paradigm particularly sensitive to the interaction between optimization constraints (e.g., KL regularization) and the pre-trained representation geometry, where overly aggressive updates can collapse behavior or degrade general capabilities. Empirically, strong gains can emerge from modifying only a small fraction of parameters (Mukherjee et al., 2025), and mechanistic studies suggest that effective RLVR updates are geometrically biased to preserve the pre-trained structure (Zhu et al., 2025; Cai et al., 2025).

However, current PEFT methodologies encounter significant obstacles when applied to the RLVR paradigm. Firstly, SVD-based low-rank adaptation methods are constrained by a severe geometric dimension mismatch (Yin et al., 2025). PiSSA (Meng et al., 2024), for instance, creates a structural conflict by forcing updates on principal components; this directly violates RLVR’s preference for updating non-principal components to protect principal features. Conversely, while MiLoRA (Wang et al., 2025) attempts to accommodate this geometric property by initializing minor components, it fails due to weak initialization amplitudes, leading to optimization collapse where the model rapidly retreats to the principal subspace. Secondly, sparse fine-tuning (Mukherjee et al., 2025; Zhu et al., 2025) methods designed to exploit RL update patterns struggle with computational efficiency. Due to a lack of modern hardware support for unstructured sparsity, these methods fail to convert theoretical sparsity into real-world speedups. Consequently, the additional overhead often exacerbates, rather than alleviates, the computational burden.

To this end, we introduce **GeoRA** (Geometry-

[†] Work done during internship at Meituan

[‡] Corresponding authors

^{*} Equal contribution

Aware Low-Rank Adaptation). Our analysis reveals that the RLVR update subspace is not isotropic but possesses a distinct low-rank structure. Leveraging this, GeoRA extracts dominant trainable directions directly from this subspace for initialization, while keeping residual components frozen to preserve knowledge. This approach achieves a dual advantage: it geometrically aligns with RLVR’s optimization dynamics and inherently preserves dense matrix compatibility, thereby delivering high computational efficiency without the overhead of sparse methods. To the best of our knowledge, GeoRA is the first geometry-based low-rank adaptation framework explicitly tailored to RLVR’s distinctive optimization dynamics. Our contributions are summarized as follows:

- We propose GeoRA, a geometry-aware, low-rank, and parameter-efficient adaptation framework tailored to RLVR. By aligning low-rank adaptation with RLVR’s distinctive optimization dynamics, GeoRA mitigates spectral mismatch and enables stable training.
- We show that the effective RL update subspace is directional and admits a compressible low-rank structure. GeoRA extracts principal trainable directions via SVD within this subspace to initialize low-rank adapters, while a frozen residual component acts as a structural anchor to preserve pre-trained knowledge.
- Experiments on Qwen and Llama models demonstrate that GeoRA improves stability and consistently outperforms leading low-rank baselines on multiple mainstream mathematical benchmarks, while exhibiting superior robustness on out-of-distribution tasks.

2 Related Work

2.1 RLVR and Optimization Geometry

RLVR replaces traditional reward models with deterministic verifiers (e.g., in math or coding) (Zhang et al., 2025; Lambert et al., 2025; Yuan et al., 2025). Through outcome-based feedback, it incentivizes emergent reasoning behaviors like Chain-of-Thought (CoT), establishing itself as a core paradigm for enhancing LLM reasoning (Hu et al., 2025; Liu et al., 2025a).

Recent mechanistic analyses have delineated a sharp dichotomy between supervised fine-tuning (SFT) and reinforcement learning with verifiable

rewards (RLVR). While SFT primarily injects knowledge by modifying principal weight directions (Chu et al., 2025; Jin et al., 2025b), RLVR is better characterized as a constrained optimization process (Wu et al., 2025) that amplifies latent reasoning behaviors via reward-induced sampling bias rather than introducing new capabilities (Yue et al., 2025; Zhao et al.; Alam and Rastogi, 2025). Theoretically, these updates manifest “off the principals,” favoring low-magnitude directions orthogonal to pre-trained features (Zhu et al., 2025), consistent with the rank-1 dominance observed in early training (Cai et al., 2025). However, this regime faces stability trade-offs. KL-regularization (“RL’s Razor”) attempts to limit forgetting (Shenfeld et al., 2025) but can precipitate the “Reasoning Boundary Paradox,” where aggressive reward maximization collapses exploration diversity (Nguyen et al., 2025). Although capability degradation may be partially reversed via singular vector rotation (Jin et al., 2025a,b), adaptation remains fundamentally constrained by the “Invisible Leash,” which enforces proximity to the pre-training manifold (Wu et al., 2025). Empirically, strong gains can emerge from updating only a small fraction of parameters, suggesting that RL fine-tuning often concentrates on small subnetworks (Mukherjee et al., 2025).

2.2 PEFT and Spectral Priors

To alleviate the computational demands of scaling LLMs, PEFT (Xu et al., 2023; Han et al., 2024) has emerged as a key paradigm, minimizing memory overhead by updating only a fraction of parameters while matching full fine-tuning performance. Prevailing strategies include partial fine-tuning (Zaken et al., 2022; Lawton et al., 2023), soft prompt tuning (Hambardzumyan et al., 2021), non-linear adapters (Lin et al., 2020), low-rank adaptation (Li et al., 2018), and importance-aware methods like LIFT (Liu et al., 2025b).

Among these, LoRA (Hu et al., 2022) and its variants are the de facto standard, yet their initialization strategies often diverge based on spectral priors. For instance, PiSSA (Meng et al., 2024) allocates trainable parameters to principal singular components, imposing a strong inductive bias validated primarily in SFT. However, such SFT-oriented spectral priors can create a fundamental geometric mismatch in RLVR, whose optimization dynamics and effective update patterns differ markedly from SFT (Yin et al., 2025; Zhu et al., 2025; Mukherjee et al., 2025). MiLoRA (Wang

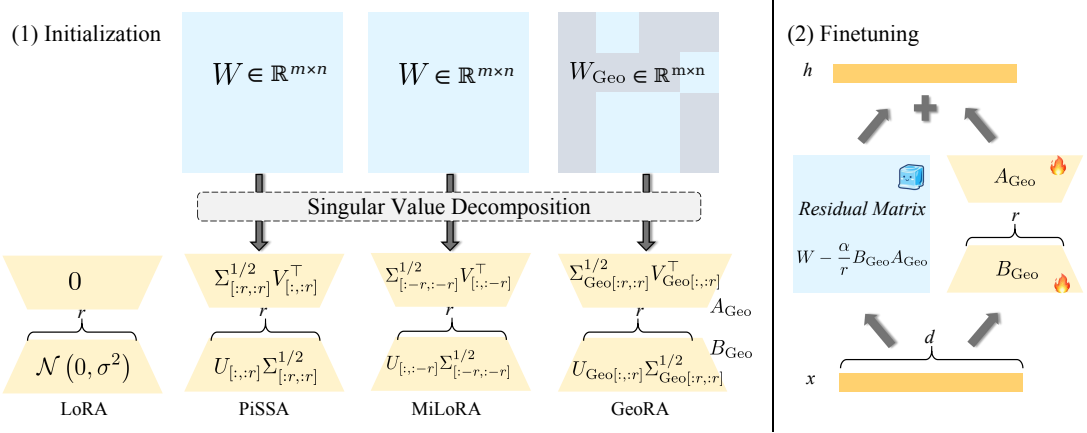


Figure 1: Comparison of adapter initialization and forward architectures. **LoRA** applies low-rank adaptation on the original weight matrix W with standard initialization, while **PiSSA** initializes adapters from the principal components of W . In contrast, **GeoRA** initializes from a geometry-constrained matrix W_{Geo} (a different adaptation target than W). Its forward pass incorporates a frozen Residual Matrix in parallel with the trainable adapter to act as a stability anchor for principal components.

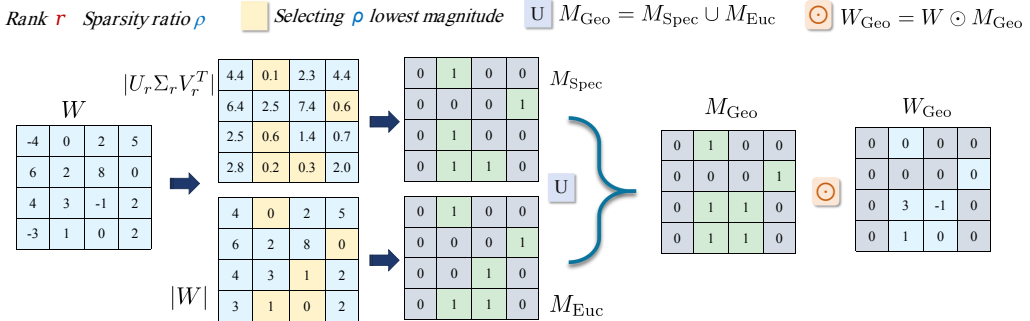


Figure 2: Geometric Prior Construction via Masking. The process of generating M_{Geo} by combining Spectral Priors (low-curvature regions) and Euclidean Priors (high-plasticity near-zero weights). The resulting W_{Geo} isolates the most stable parameters for RL-native adaptation.

et al., 2025) instead targets minor components, but does not explicitly account for RLVR-specific geometry and dynamics. Other variants like DoRA (Liu et al., 2024), AdaLoRA (Zhang et al., 2023), and VeRA (Kopczko et al., 2023) focus on weight decomposition or budget allocation without integrating these RLVR-native geometric considerations. Building on these observations, GeoRA translates RLVR-specific mechanistic insights into an actionable PEFT paradigm.

3 Methodology

We introduce **GeoRA** (Geometry-Aware Low-Rank Adaptation), a low-rank adaptation framework tailored for RLVR. GeoRA emphasizes an RL-native, structured low-rank parameterization together with an explicit residual leash for stability. Comparing with SFT-oriented PEFT baselines like LoRA and PiSSA, we first present the low-rank for-

ward architecture and initialization (Figure 1), and then describe a lightweight masking instantiation that constructs the geometry-constrained matrix used for initialization (Figure 2).

3.1 Geometry-Aware Low-Rank Structure

Let W_{Geo} denote a geometry-constrained view of the pre-trained weight matrix W . Unlike standard LoRA which initializes adapters randomly (or with zero), GeoRA leverages the compressible structure within W_{Geo} to derive a structured initialization.

We first perform Singular Value Decomposition (SVD) on the geometry-constrained matrix:

$$W_{\text{Geo}} = U_{\text{Geo}} \Sigma_{\text{Geo}} V_{\text{Geo}}^T \quad (1)$$

We extract the top- r singular components that capture the principal geometric information. The low-rank adapters A_{Geo} and B_{Geo} are then initialized to approximate this geometry-aware subspace:

$$A_{\text{Geo}} = \Sigma_{\text{Geo}[:,r,:r]}^{1/2} V_{\text{Geo}[:,r,:]}^\top \quad (2)$$

$$B_{\text{Geo}} = U_{\text{Geo}[:,:r,:r]} \Sigma_{\text{Geo}[:,r,:r]}^{1/2} \quad (3)$$

By this design, the initial product $B_{\text{Geo}} A_{\text{Geo}}$ constructs the rank- r approximation of W_{Geo} .

Crucially, to ensure the model’s output remains unchanged at initialization and to preserve core capabilities during training, we follow the standard LoRA scaling and compute a Residual Matrix W_{res} by subtracting the scaled initialized adapters from the original weights:

$$W_{\text{res}} = W - \frac{\alpha}{r} B_{\text{Geo}} A_{\text{Geo}} \quad (4)$$

During the forward pass, W_{res} is kept **frozen**. The hidden state h is computed as:

$$h = \underbrace{W_{\text{res}} x}_{\text{Frozen}} + \underbrace{\frac{\alpha}{r} B_{\text{Geo}} A_{\text{Geo}} x}_{\text{Trainable}} \quad (5)$$

This construction keeps the model function-preserving at initialization (since $W_{\text{res}} x + \frac{\alpha}{r} B_{\text{Geo}} A_{\text{Geo}} x = W x$) and enforces a hard structural constraint: the optimizer can only update the geometry-aligned manifold parameterized by A_{Geo} and B_{Geo} , while W_{res} acts as a stability anchor preventing the erosion of pre-trained representations.

3.2 Geometric Prior Construction

To instantiate a geometry-aware update region, we construct a geometry-constrained matrix W_{Geo} using a masking strategy. This masking is consistent with prior observations on spectral and magnitude structure and stability in fine-tuning (Liu et al., 2025b; Zhu et al., 2025).

The Spectral Prior (M_{Spec}) promotes geometric stability by selecting the bottom ρ -fraction of entries from the rank- r approximation \hat{W}_r . The mask is defined as:

$$(M_{\text{Spec}})_{i,j} = \mathbb{I}(|(\hat{W}_r)_{i,j}| \leq \tau_{\text{Spec}}(\rho)) \quad (6)$$

where $\tau_{\text{Spec}}(\rho)$ is the ρ -th quantile of the absolute values in \hat{W}_r . Intuitively, this mask suppresses high-magnitude (and typically high-curvature) components and constrains updates to a more stable, low-magnitude region, improving spectral stability under RLVR. Similarly, the Euclidean Prior (M_{Euc}) selects low-magnitude weights to capture

parameter plasticity, using the same sparsity ratio ρ :

$$(M_{\text{Euc}})_{i,j} = \mathbb{I}(|W_{i,j}| \leq \tau_{\text{Euc}}(\rho)) \quad (7)$$

Here, $\tau_{\text{Euc}}(\rho)$ represents the ρ -th quantile of $|W|$. The final geometry-constrained matrix W_{Geo} is formed by the **union** of these two stable subspaces:

$$W_{\text{Geo}} = W \odot (M_{\text{Spec}} \cup M_{\text{Euc}}) \quad (8)$$

This union ensures that the optimized weights retain the flexibility of small parameters while respecting the spectral constraints of the pre-trained model.

4 Experiments

4.1 Main Results and Efficiency

We conduct a comprehensive performance comparison of GeoRA against MiLoRA (Wang et al., 2025), PiSSA (Meng et al., 2024), LoRA (Hu et al., 2022), Sparse Fine-Tuning (SparseFT, based on $2M_{\text{Geo}}$ masking), and Full Fine-Tuning (FullFT). In our experiments, we fine-tune Qwen3-8B-Base (Yang et al., 2025) and Llama-3.1-8B-Instruct (Dubey et al., 2024) on the DeepMath-103K dataset (He et al., 2025) using the GRPO algorithm (Shao et al., 2024), with a fixed rank $r = 16$ and sparsity ratio $\rho = 0.2$. We use both base and instruction-tuned backbones to reflect robustness across model variants. We evaluate their In-Distribution (ID) problem-solving capabilities on MATH-500 (Hendrycks et al., 2021), AIME (Patel et al., 2024), and OlymMATH (Sun et al., 2025). Furthermore, to assess the preservation of general capabilities and cross-domain generalization, we conduct evaluations on Out-of-Distribution (OOD) benchmarks, including HumanEval (Coding) (Chen, 2021), GPQA (Science) (Rein et al., 2024), and MMLU (General Knowledge) (Hendrycks et al., 2020).

Mathematical Reasoning Performance. Table 1 shows that GeoRA achieves the highest average scores on both Qwen3-8B and Llama-3.1 (34.04 and 24.51, respectively). GeoRA establishes a new state-of-the-art (SOTA) among PEFT methods and further surpasses Full Fine-Tuning (FullFT) and Sparse Fine-Tuning (SparseFT). Notably, on challenging competition-level benchmarks such as AIME and OlymMATH, GeoRA demonstrates superior performance, significantly outperforming LoRA, MiLoRA, and PiSSA. This suggests that the geometric initialization strategy

Table 1: Comprehensive performance comparison on In-Distribution (ID) and Out-of-Distribution (OOD) tasks.

Method	In-Distribution (ID)					Out-of-Distribution (OOD)		
	AIME24	AIME25	MATH500	OlymMATH	Avg.	HumanEval	GPQA	MMLU
<i>Qwen3-8B</i>								
FullFT	23.33	22.08	78.40	11.25	33.77	76.83	36.91	71.94
SparseFT	22.92	21.25	76.80	11.50	33.12	79.50	37.20	74.20
LoRA	19.58	19.58	75.60	10.75	31.38	81.10	37.50	75.65
PiSSA	22.50	20.42	74.40	11.75	32.27	71.95	36.16	73.89
MiLoRA	20.42	19.58	76.20	11.50	31.93	78.66	38.26	74.51
GeoRA	23.75	21.67	78.00	12.75	34.04	82.93	<u>37.92</u>	75.96
<i>Llama-3.1-8B</i>								
FullFT	18.33	8.25	62.40	8.50	24.37	65.20	31.15	68.40
SparseFT	17.92	<u>8.10</u>	61.50	8.25	23.94	67.80	31.65	69.10
LoRA	15.42	6.25	58.20	6.75	21.66	69.80	<u>32.10</u>	69.80
PiSSA	17.50	7.92	60.50	7.75	23.42	67.50	31.80	69.20
MiLoRA	16.25	7.08	59.10	7.25	22.42	68.20	32.00	<u>70.50</u>
GeoRA	18.54	8.75	<u>61.90</u>	8.85	24.51	70.80	32.65	70.95

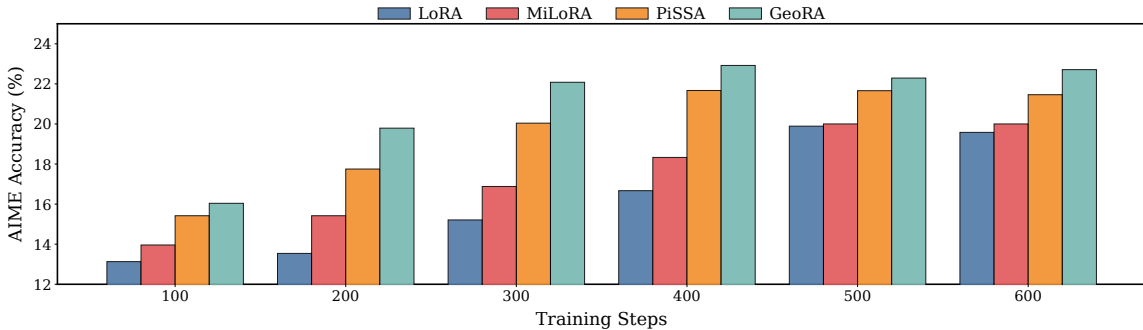


Figure 3: Training dynamics of Qwen3-8B on the AIME benchmark (average of 2024 and 2025). GeoRA remains consistently top-performing throughout training.

Table 2: Efficiency Comparison between Full FT, SparseFT, and GeoRA, displaying absolute metrics (top) and relative reductions vs. Full FT (bottom).

Method	Params (B)	Time (s/it)	VRAM (%)
Full FT	8.00	231	95.73
SparseFT	2.56 (-68.0%)	256 (+10.8%)	81.25 (-15.1%)
GeoRA	0.04 (-99.5%)	185 (-19.9%)	68.43 (-28.5%)

navigates the optimization landscape more effectively than random or magnitude-based initializations, enabling superior convergence even with minimal parameter updates.

Generalization and Forgetting Resistance. GeoRA exhibits remarkable robustness against

"catastrophic forgetting" (Table 1, right). In contrast to FullFT, which causes a substantial degradation in Qwen3's coding capabilities (dropping to 76.83), GeoRA maintains a high score of 82.93 on HumanEval and achieves the best results on both MMLU and GPQA. This demonstrates that by selectively updating only the "safe" geometric subspaces, GeoRA enhances mathematical reasoning without disrupting pre-existing general knowledge structures.

Training Dynamics and Efficiency. Figure 3 reveals that GeoRA converges faster and more stably, identifying a strictly dominant trajectory where it reaches performance levels at step 300 that other PEFT methods struggle to attain even at step 600. Regarding efficiency (Table 2), GeoRA reduces trainable parameters by 99.5% and VRAM usage by 28.5% compared to FullFT, while im-

Method	Reward	AIME24	AIME25	MATH-500	OlymMATH	Avg.
GeoRA	0.88	13.33	9.17	73.40	5.75	25.41
<i>Ablation on Initialization Strategy</i>						
Random- r Init	0.85	12.50	8.50	72.10	5.25	24.60
Tail- r Init	0.82	11.67	7.50	70.80	4.50	23.40
<i>Ablation on Geometric Masks</i>						
w/o M_{Spec}	0.86	12.50	8.33	72.00	4.75	24.40
w/o M_{Euc}	0.83	13.33	8.75	72.80	5.50	25.10

Table 3: Comprehensive ablation study on Initialization Strategies and Geometric Masks. We evaluate the impact of different initialization methods (Random- r , Tail- r) and the removal of specific mask components (M_{Spec} , M_{Euc}). The results demonstrate that the full GeoRA model consistently achieves superior performance across all benchmarks.

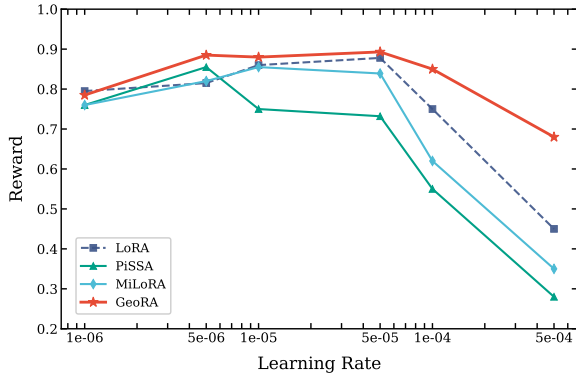


Figure 4: **Performance comparison across different learning rates.** Unlike baselines, GeoRA demonstrates superior stability and robust convergence even at higher learning rates.

proving training speed by 19.9%. Crucially, this speedup empirically validates our design choice: by strictly preserving dense matrix compatibility, GeoRA successfully bypasses the hardware overhead associated with unstructured sparsity (e.g., dynamic masking) present in SparseFT, translating theoretical hardware-friendliness into tangible computational acceleration.

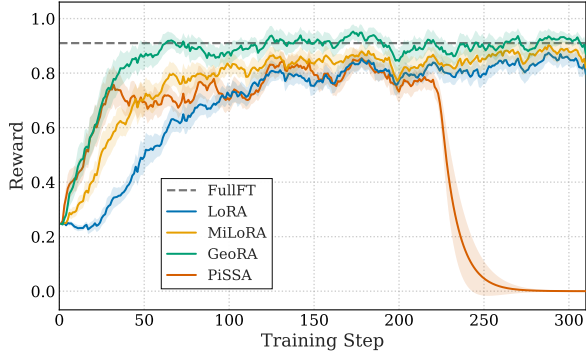
4.2 Ablation Studies and Robustness Analysis

In this section, we conduct a comprehensive analysis to verify the effectiveness of individual components and the stability of our proposed method. To ensure a controlled and efficient evaluation, all experiments in this section are conducted using the Qwen3-4B-Base (Yang et al., 2025) model, optimized via GRPO on the GSM8K (Cobbe et al., 2021) dataset.

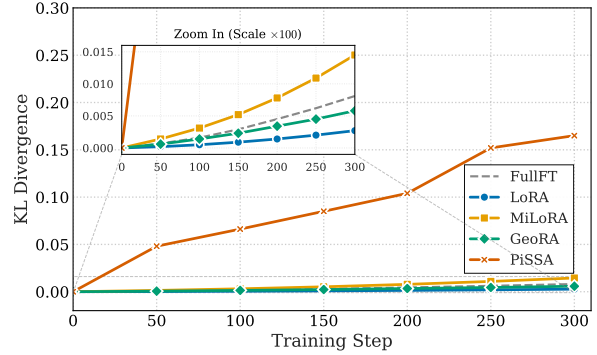
Impact of Initialization Strategies. One of the core contributions of GeoRA is the utilization of a geometric prior to initialize trainable parameters.

To validate the necessity of this strategy, we compare three distinct initialization methods in Table 3: (1) GeoRA, which initializes using the top- r principal components of W_{Geo} ; (2) Random- r Init, which initializes the low-rank adapters with a random Gaussian distribution; and (3) Tail- r Init, which initializes using the bottom- r components (tail components) derived from the singular value decomposition (SVD) of W_{Geo} . The experimental results demonstrate that GeoRA’s initialization strategy achieves the best performance (Avg 25.41, Reward 0.88). In comparison, Random- r Init exhibits a slight performance degradation (Avg 24.60). This suggests that while random initialization is effective for standard LoRA, the lack of prior information hinders optimization under sparse geometric constraints. More importantly, Tail- r Init performs the worst (Avg 23.40). This confirms our hypothesis that the “tail” components of the weights primarily consist of noise or redundant information; utilizing these components for initialization is not only unbeneficial but actually interferes with the model’s ability to learn critical features. Therefore, leveraging the principal components (Head) of W_{Geo} is essential for maintaining high performance in extremely low-parameter regimes.

Training Stability. Training instability remains a notorious bottleneck in RL fine-tuning, typically manifesting as abrupt performance degradation or catastrophic reward collapse. We hypothesize that this stems from a fundamental geometric mismatch: PiSSA enforces updates along principal components—directions often associated with high curvature—which is prone to violating the trust region constraint ($D_{KL} < \delta$) essential for stable RLVR. To validate this, Figure 5 presents a stress test conducted under an aggressive learning rate



(a) Reward Trajectories



(b) KL Divergence

Figure 5: **Training Stability and Constraint Adherence.** Under aggressive learning rates (5×10^{-5}), **GeoRA** demonstrates superior robustness.

(5×10^{-5}). As illustrated in Figure 5(a), PiSSA suffers a catastrophic reward collapse around step 220. Crucially, Figure 5(b) uncovers the root cause: this collapse coincides with an explosive surge in KL divergence, indicating that the model has violated optimization constraints and drifted into a degenerate policy space. In stark contrast, GeoRA demonstrates three distinct advantages rooted in its geometric alignment: (1) Superior Optimality: It establishes a significantly higher *performance envelope* (green curve), indicating more effective exploration of the reasoning manifold compared to all baselines. (2) Intrinsic Stability: It remains immune to collapse, effectively filtering out the destabilizing updates that plague spectrum-misaligned methods. (3) Constraint Adherence: It achieves these gains while maintaining a flat, controlled KL divergence profile. This confirms that GeoRA’s geometry-aware subspace functions as a natural regularizer, enabling the model to maximize rewards strictly within the safe trust region of the pre-trained backbone.

Furthermore, extensive experiments were conducted to validate the model multidimensionally. As shown in Figure 4, since instability is often amplified by overly large learning rates, a broad sweep of learning rates attests to GeoRA’s superior stability, ensuring robust convergence where baselines collapse; and parameter sensitivity analysis underscores the model’s resilience, demonstrating competitive performance even under extreme conditions such as ultra-low rank (4) or high sparsity (10%).

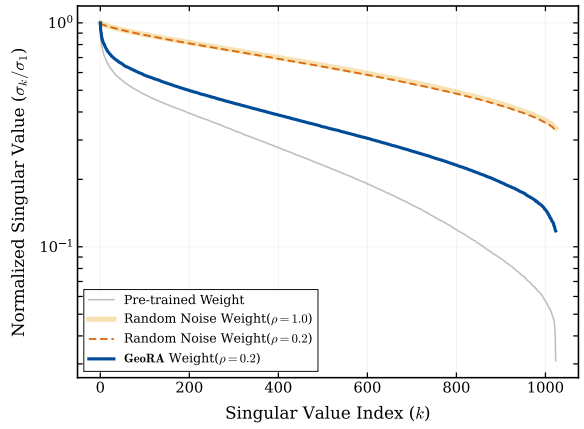


Figure 6: Singular Value Spectrum Analysis. The visualization is based on W_k at Layer 33 of the Qwen3-8B model.

5 Mechanism Analysis

To reveal the geometric origins of GeoRA’s superior balance between enhancing in-domain (ID) tasks and preserving out-of-domain (OOD) capabilities, we conduct a quantitative mechanism analysis.

5.1 Intrinsic Low-Rank Structure of Updates

To validate the structural foundation of GeoRA, we investigate the physical compressibility of learned updates. We analyze the singular value spectrum of the GeoRA update matrix W_{Geo} and compare it against the original pre-trained weights, as well as random noise matrices at both full density ($\rho = 1.0$) and sparse density ($\rho = 0.2$). Figure 6 reveals two critical insights that challenge conventional assumptions in sparse fine-tuning:

- **Sparsity \neq Low-Rankness (The Isotropic Fallacy):** A notable observation is that the

Method	Llama-3.1-8B			Qwen3-8B		
	NSS \downarrow	$\mathcal{S}_{\text{Head}} \downarrow$	$\mathcal{S}_{\text{Tail}} \uparrow$	NSS \downarrow	$\mathcal{S}_{\text{Head}} \downarrow$	$\mathcal{S}_{\text{Tail}} \uparrow$
PiSSA	0.395	0.98	0.01	0.418	0.95	0.03
LoRA	0.214	0.15	0.15	0.235	0.18	0.18
MiLoRA	0.125	0.12	0.92	0.132	0.16	0.90
GeoRA	0.092	0.005	0.98	0.096	0.015	0.96

Table 4: Geometric Mechanism Analysis.

spectrum of sparse random noise ($\rho = 0.2$) almost perfectly overlaps with that of dense random noise ($\rho = 1.0$). Both exhibit a gentle, slowly decaying trajectory, indicating an isotropic (high-rank) distribution of energy. This proves that unstructured sparsity alone fails to induce true geometric structure; in the spectral domain, a sparse random mask is mathematically equivalent to high-entropy white noise.

- **Inheritance of Pre-trained Geometry:** In sharp contrast, the GeoRA update subspace W_{Geo} retains the characteristic power-law decay of the original pre-trained weights, concentrating the vast majority of information in a few top singular components. This confirms that effective RL updates are not random, but align with the compressible, low-rank structure of the pre-trained model.

This spectral analysis provides the theoretical justification for GeoRA: Since the optimal update subspace is intrinsically low-rank rather than sparsely random, we can replace inefficient unstructured sparsity with SVD-based initialization. This transforms the optimization into efficient dense parameterization, ensuring rigorous geometric alignment while maximizing computational efficiency.

5.2 Spectral Efficiency and Alignment

Building on the low-rank structure of RL updates, we validate GeoRA’s geometric superiority via **Normalized Spectral Shift (NSS)** and **Subspace Alignment** (Table 4). First, NSS quantifies the topological distortion of the pre-trained manifold:

$$\text{NSS} = \frac{\|\sigma(W^{\text{tuned}}) - \sigma(W)\|_2}{\|\sigma(W)\|_2}. \quad (9)$$

While PiSSA exhibits high NSS (> 0.39), indicating aggressive structural modification, GeoRA maintains minimal distortion (≈ 0.09), confirming

it maximizes reward acquisition while preserving fundamental features.

To pinpoint the update locus, we calculate the alignment between ΔW and the pre-trained singular vectors V :

$$\mathcal{S}(k) = \frac{\|\Delta W v_k\|_2}{\|\Delta W\|_F} \approx |\cos(\theta_k)|. \quad (10)$$

GeoRA shows a distinct signature: it avoids the high-energy principal subspace ($\mathcal{S}_{\text{Head}} \leq 0.02$)—enhancing stability—and efficiently adapts the geometry-constrained tail ($\mathcal{S}_{\text{Tail}} \geq 0.96$). In contrast, PiSSA’s instability is explained by its high overlap with the head subspace (≈ 0.98).

6 Conclusion

In this paper, we bridge the gap between PEFT and the unique optimization dynamics of RLVR. Our investigation suggests that the instability often observed in RL fine-tuning arises from a structural mismatch: SFT-centric methods (e.g., PiSSA) prioritize principal components that may misalign with the geometry-constrained updates required by RLVR. GeoRA addresses this by identifying a compressible, geometry-aligned update subspace and parameterizing it via structured SVD initialization with a residual leash. Extensive evaluations confirm that GeoRA offers a robust solution for deploying large reasoning models, demonstrating exceptional stability under aggressive training conditions and superior generalization on out-of-distribution tasks. By reconciling the plasticity required for policy improvement with the structural integrity of the foundation model, GeoRA establishes a new standard for efficient and stable RLVR.

Limitations

Despite its effectiveness, GeoRA has certain limitations. First, the initialization process requires performing a truncated SVD and dual-masking operations. While these represent a one-time computational cost at the beginning of training, they

introduce an additional pre-processing step compared to the random initialization used in standard LoRA. Second, our experiments primarily focus on RLVR in reasoning domains. Although GeoRA demonstrates strong performance on these tasks, its generalizability needs to be further validated across a broader range of model architectures and diverse reinforcement learning scenarios beyond verifiable rewards.

References

Md Tanvirul Alam and Nidhi Rastogi. 2025. Limits of generalization in rlvr: Two case studies in mathematical reasoning. *arXiv preprint arXiv:2510.27044*.

Yuchen Cai, Ding Cao, Xin Xu, Zijun Yao, Yuqing Huang, Zhenyu Tan, Benyi Zhang, Guiquan Liu, and Junfeng Fang. 2025. On predictability of reinforcement learning dynamics for large language models. *arXiv preprint arXiv:2510.00553*.

Mark Chen. 2021. Evaluating large language models trained on code. *arXiv preprint arXiv:2107.03374*.

Tianzhe Chu, Yuexiang Zhai, Jihan Yang, Shengbang Tong, Saining Xie, Dale Schuurmans, Quoc V Le, Sergey Levine, and Yi Ma. 2025. Sft memorizes, rl generalizes: A comparative study of foundation model post-training. *arXiv preprint arXiv:2501.17161*.

Karl Cobbe, Vineet Kosaraju, Mohammad Bavarian, Mark Chen, Heewoo Jun, Lukasz Kaiser, Matthias Plappert, Jerry Tworek, Jacob Hilton, Reiichiro Nakano, and 1 others. 2021. Training verifiers to solve math word problems. *arXiv preprint arXiv:2110.14168*.

Abhimanyu Dubey, Abhinav Jauhri, Abhinav Pandey, Abhishek Kadian, Ahmad Al-Dahle, Aiesha Letman, Akhil Mathur, Alan Schelten, Amy Yang, Angela Fan, and 1 others. 2024. The llama 3 herd of models. *arXiv preprint arXiv:2407.21783*.

Daya Guo, Dejian Yang, Haowei Zhang, Junxiao Song, Ruoyu Zhang, Runxin Xu, Qihao Zhu, Shirong Ma, Peiyi Wang, Xiao Bi, and 1 others. 2025. Deepseek-r1: Incentivizing reasoning capability in llms via reinforcement learning. *arXiv preprint arXiv:2501.12948*.

Karen Hambardzumyan, Hrant Khachatrian, and Jonathan May. 2021. Warp: Word-level adversarial reprogramming. *arXiv preprint arXiv:2101.00121*.

Zeyu Han, Chao Gao, Jinyang Liu, Jeff Zhang, and Sai Qian Zhang. 2024. Parameter-efficient fine-tuning for large models: A comprehensive survey. *arXiv preprint arXiv:2403.14608*.

Zhiwei He, Tian Liang, Jiahao Xu, Qiuzhi Liu, Xingyu Chen, Yue Wang, Linfeng Song, Dian Yu, Zhenwen Liang, Wenxuan Wang, and 1 others. 2025. Deepmath-103k: A large-scale, challenging, decontaminated, and verifiable mathematical dataset for advancing reasoning. *arXiv preprint arXiv:2504.11456*.

Dan Hendrycks, Collin Burns, Steven Basart, Andy Zou, Mantas Mazeika, Dawn Song, and Jacob Steinhardt. 2020. Measuring massive multitask language understanding. *arXiv preprint arXiv:2009.03300*.

Dan Hendrycks, Collin Burns, Saurav Kadavath, Akul Arora, Steven Basart, Eric Tang, Dawn Song, and Jacob Steinhardt. 2021. Measuring mathematical problem solving with the math dataset. *arXiv preprint arXiv:2103.03874*.

Edward J Hu, Yelong Shen, Phillip Wallis, Zeyuan Allen-Zhu, Yuanzhi Li, Shean Wang, Lu Wang, Weizhu Chen, and 1 others. 2022. Lora: Low-rank adaptation of large language models. *ICLR*, 1(2):3.

Jingcheng Hu, Yinmin Zhang, Qi Han, Dixin Jiang, Xiangyu Zhang, and Heung-Yeung Shum. 2025. Openreasoner-zero: An open source approach to scaling up reinforcement learning on the base model. *arXiv preprint arXiv:2503.24290*.

Aaron Jaech, Adam Kalai, Adam Lerer, Adam Richardson, Ahmed El-Kishky, Aiden Low, Alec Helyar, Aleksander Madry, Alex Beutel, Alex Carney, and 1 others. 2024. Openai o1 system card. *arXiv preprint arXiv:2412.16720*.

Hangzhan Jin, Sitao Luan, Sicheng Lyu, Guillaume Rabusseau, Reihaneh Rabbany, Doina Precup, and Mohammad Hamdaqa. 2025a. Rl fine-tuning heals ood forgetting in sft. *arXiv preprint arXiv:2509.12235*.

Hangzhan Jin, Sicheng Lv, Sifan Wu, and Mohammad Hamdaqa. 2025b. Rl is neither a panacea nor a mirage: Understanding supervised vs. reinforcement learning fine-tuning for llms. *arXiv preprint arXiv:2508.16546*.

Dawid J Kopiczko, Tijmen Blankevoort, and Yuki M Asano. 2023. Vera: Vector-based random matrix adaptation. *arXiv preprint arXiv:2310.11454*.

Nathan Lambert, Jacob Morrison, Valentina Pyatkin, Shengyi Huang, H Ivison, F Brahman, LJV Miranda, A Liu, N Dziri, S Lyu, and 1 others. 2025. Tulu 3: Pushing frontiers in open language model post-training, 2024. *URL https://arxiv.org/abs/2411.15124, 297*.

Neal Lawton, Anoop Kumar, Govind Thattai, Aram Galstyan, and Greg Ver Steeg. 2023. Neural architecture search for parameter-efficient fine-tuning of large pre-trained language models. In *Findings of the Association for Computational Linguistics: ACL 2023*, pages 8506–8515.

Chunyuan Li, Heerad Farkhoor, Rosanne Liu, and Jason Yosinski. 2018. Measuring the intrinsic dimension of objective landscapes. *arXiv preprint arXiv:1804.08838*.

Zhaojiang Lin, Andrea Madotto, and Pascale Fung. 2020. Exploring versatile generative language model via parameter-efficient transfer learning. *arXiv preprint arXiv:2004.03829*.

Mingjie Liu, Shizhe Diao, Ximing Lu, Jian Hu, Xin Dong, Yejin Choi, Jan Kautz, and Yi Dong. 2025a. Prorl: Prolonged reinforcement learning expands reasoning boundaries in large language models. *arXiv preprint arXiv:2505.24864*.

Shih-Yang Liu, Chien-Yi Wang, Hongxu Yin, Pavlo Molchanov, Yu-Chiang Frank Wang, Kwang-Ting Cheng, and Min-Hung Chen. 2024. Dora: Weight-decomposed low-rank adaptation. In *Forty-first International Conference on Machine Learning*.

Zihang Liu, Tianyu Pang, Oleg Balabanov, Chaoqun Yang, Tianjin Huang, Lu Yin, Yaoqing Yang, and Shiwei Liu. 2025b. Lift the veil for the truth: Principal weights emerge after rank reduction for reasoning-focused supervised fine-tuning. *arXiv preprint arXiv:2506.00772*.

Fanxu Meng, Zhaohui Wang, and Muhan Zhang. 2024. Pissa: Principal singular values and singular vectors adaptation of large language models. *Advances in Neural Information Processing Systems*, 37:121038–121072.

Sagnik Mukherjee, Lifan Yuan, Dilek Hakkani-Tur, and Hao Peng. 2025. Reinforcement learning finetunes small subnetworks in large language models. *arXiv preprint arXiv:2505.11711*.

Phuc Minh Nguyen, Chinh D La, Duy MH Nguyen, Nitesh V Chawla, Binh T Nguyen, and Khoa D Doan. 2025. The reasoning boundary paradox: How reinforcement learning constrains language models. *arXiv preprint arXiv:2510.02230*.

Bhrij Patel, Souradip Chakraborty, Wesley A Suttle, Mengdi Wang, Amrit Singh Bedi, and Dinesh Manocha. 2024. Aime: Ai system optimization via multiple llm evaluators. *arXiv preprint arXiv:2410.03131*.

David Rein, Betty Li Hou, Asa Cooper Stickland, Jackson Petty, Richard Yuanzhe Pang, Julien Dirani, Julian Michael, and Samuel R Bowman. 2024. Gpqa: A graduate-level google-proof q&a benchmark. In *First Conference on Language Modeling*.

Zhihong Shao, Peiyi Wang, Qihao Zhu, Runxin Xu, Junxiao Song, Xiao Bi, Haowei Zhang, Mingchuan Zhang, YK Li, Yang Wu, and 1 others. 2024. Deepseekmath: Pushing the limits of mathematical reasoning in open language models. *arXiv preprint arXiv:2402.03300*.

Idan Shenfeld, Jyothish Pari, and Pulkit Agrawal. 2025. RL’s razor: Why online reinforcement learning forgets less. *arXiv preprint arXiv:2509.04259*.

Haoxiang Sun, Yingqian Min, Zhipeng Chen, Wayne Xin Zhao, Lei Fang, Zheng Liu, Zhongyuan Wang, and Ji-Rong Wen. 2025. Challenging the boundaries of reasoning: An olympiad-level math benchmark for large language models. *arXiv preprint arXiv:2503.21380*.

Hanqing Wang, Yixia Li, Shuo Wang, Guanhua Chen, and Yun Chen. 2025. Milora: Harnessing minor singular components for parameter-efficient llm fine-tuning. In *Proceedings of the 2025 Conference of the Nations of the Americas Chapter of the Association for Computational Linguistics: Human Language Technologies (Volume 1: Long Papers)*, pages 4823–4836.

Fang Wu, Weihao Xuan, Ximing Lu, Mingjie Liu, Yi Dong, Zaid Harchaoui, and Yejin Choi. 2025. The invisible leash: Why rlvr may or may not escape its origin. *arXiv preprint arXiv:2507.14843*.

Lingling Xu, Haoran Xie, Si-Zhao Joe Qin, Xiaohui Tao, and Fu Lee Wang. 2023. Parameter-efficient fine-tuning methods for pretrained language models: A critical review and assessment. *arXiv preprint arXiv:2312.12148*.

An Yang, Anfeng Li, Baosong Yang, Beichen Zhang, Binyuan Hui, Bo Zheng, Bowen Yu, Chang Gao, Chengan Huang, Chenxu Lv, and 1 others. 2025. Qwen3 technical report. *arXiv preprint arXiv:2505.09388*.

Qingyu Yin, Yulun Wu, Zhennan Shen, Sunbowen Li, Zhilin Wang, Yanshu Li, Chak Tou Leong, Jiale Kang, and Jinjin Gu. 2025. Evaluating parameter efficient methods for rlvr. *arXiv preprint arXiv:2512.23165*.

Lifan Yuan, Weize Chen, Yuchen Zhang, Ganqu Cui, Hanbin Wang, Ziming You, Ning Ding, Zhiyuan Liu, Maosong Sun, and Hao Peng. 2025. From $f(x)$ and $g(x)$ to $f(g(x))$: Llms learn new skills in rl by composing old ones. *arXiv preprint arXiv:2509.25123*.

Yang Yue, Zhiqi Chen, Rui Lu, Andrew Zhao, Zhaokai Wang, Shiji Song, and Gao Huang. 2025. Does reinforcement learning really incentivize reasoning capacity in llms beyond the base model? *arXiv preprint arXiv:2504.13837*.

Elad Ben Zaken, Yoav Goldberg, and Shauli Ravfogel. 2022. Bitfit: Simple parameter-efficient fine-tuning for transformer-based masked language-models. In *Proceedings of the 60th Annual Meeting of the Association for Computational Linguistics (Volume 2: Short Papers)*, pages 1–9.

Kaiyan Zhang, Yuxin Zuo, Bingxiang He, Youbang Sun, Runze Liu, Che Jiang, Yuchen Fan, Kai Tian, Guoli Jia, Pengfei Li, and 1 others. 2025. A survey of reinforcement learning for large reasoning models. *arXiv preprint arXiv:2509.08827*.

Qingru Zhang, Minshuo Chen, Alexander Bukharin, Nikos Karampatziakis, Pengcheng He, Yu Cheng, Weizhu Chen, and Tuo Zhao. 2023. Adalora: Adaptive budget allocation for parameter-efficient fine-tuning. *arXiv preprint arXiv:2303.10512*.

Rosie Zhao, Alexandru Meterez, Sham Kakade, Cengiz Pehlevan, Samy Jelassi, and Eran Malach. Echo chamber: RL post-training amplifies behaviors learned in pretraining, 2025. *URL <https://arxiv.org/abs/2504.07912>*.

Hanqing Zhu, Zhenyu Zhang, Hanxian Huang, DiJia Su, Zechun Liu, Jiawei Zhao, Igor Fedorov, Hamed Pirsiavash, Zhizhou Sha, Jinwon Lee, and 1 others. 2025. The path not taken: RLVR provably learns off the principals. *arXiv preprint arXiv:2511.08567*.